Tool Path Generation and Manufacturing Process for Blades of a Compressor Rotor

C. Tung and P.-L. Tso

Abstract—This paper presents a complete procedure for tool path planning and blade machining in 5-axis manufacturing. The actual cutting contact and cutter locations can be determined by lead and tilt angles. The tool path generation is implemented by piecewise curved approximation and chordal deviation detection. An application about drive surface method promotes flexibility of tool control and stability of machine motion. A real manufacturing process is proposed to separate the operation into three regions with five stages and to modify the local tool orientation with an interactive algorithm.

Keywords—5-axis machining, tool orientation, lead and tilt angles, tool path generation.

I. INTRODUCTION

FIVE-AXIS machining process is wildly applied in aerospace and mold industries due to the advantages of high quality and efficiency. A compressor rotor namely the impeller is one of the most representative and difficult-producing workpiece with sculptured surface [1]–[3].

Machining this type of products requires a high degree of flexibility in tool orientation. There are many researches in determining the lead and tilt (L/T) angles for the gauge-free tool positions [4]–[7] and stable cutting performance [8], [9]. In metal cutting, a tool must be identified for any operation. In section 2, the cutting contact (CC) point relative to the cutter location (CL) on the tool will be discussed with a generalized formula, and be determined by orientation parameters.

Tool path are generated from a set of CC points on the desired surface that are eliminated from the cutting layers on workpiece or by a series of CLs on offsetting surface. Chui, Chiu, and Yu [10] constructed a 3-dimensional (3D) biarc fitting technique for CLs to generate a 5-axis tool path. In section 3, an analytical deviation of polygonal approximation is introduced to determine the step-length increments for path computation.

Cutting cannot be performed around the tip due to zero cutting speed. Therefore the tool needs to be tilted relative to the surface normal. Tool interference is the key constraint to accurate machining. In section 4, a principle is presented to avoid local gouging when the cutter is placed or oriented out of the design curvature. Furthermore a drive-surface method can be applied to perform smooth control of tool orientations.

C. Tung is a PhD student with the Department of Power Mechanical Engineering, National Tsing Hua University, Hsinchu, Taiwan 30013 ROC (e-mail: jay.tung@ msa.hinet.net).

P.-L. Tso is a professor with the Department of Power Mechanical Engineering, National Tsing Hua University, Hsinchu, Taiwan 30013 ROC (phone: 886-35742919; e-mail: pltso@ pme.nthu.edu.tw).
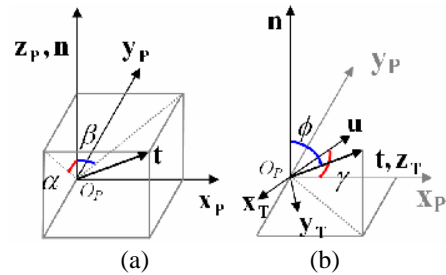
Fig. 1 Orientation relation about surface normal and tool axis

In section 5, a complete tool path is generated for machining the blades of a compressor rotor. The applications and operations of roughing, semifinishing, and finishing processes are discussed with examples.

II. TOOL ORIENTATION DETERMINATION

In sculptured surface machining, the cutter and surface curvatures are similar at the CC point. Tool axis direction is constrained by the machine movements and collision inspection. Therefore tool motion should be assigned cautiously in 5-axis machining. L/T angles are main parameters to control the cutter orientation.

As Fig. 1(a) shows, the surface normal and the tool axis are defined as **n** and **t** at each CC point. The local surface coordinate system represented by $\mathbf{x_p}\mathbf{y_p}\mathbf{z_p}$ is for each discrete CC point where $\mathbf{x_p}$ is the unit principal direction as the feed direction tangent to the tool path, $\mathbf{z_p}$ is the unit vector same with **n**, and $\mathbf{y_p} = \mathbf{z_p} \times \mathbf{x_p}$. The origin with $\mathbf{x_p}\mathbf{y_p}\mathbf{z_p}$ is located at the CC point. L/T angles represented by α and β are as the rotation angles about $\mathbf{x_p}$ and $\mathbf{y_p}$ to make **t** in the desired orientation. Lauwers, Dejonghe, and Kruth [11] had optimized the tool orientation to avoid machine collisions and to improve material removal rate. Ozturk, Tunc, and Budak [12] had experimented L/T effects to achieve better machining quality. In this paper the inclination angle ϕ between **n** and **t**, as Fig. 1(b) shows, will be introduced that could be calculated from L/T angles by trigonometric function as

$$\phi = \tan^{-1} \sqrt{\tan^2 \alpha + \tan^2 \beta} \tag{1}$$

Therefore **t** can be expressed by further parameters ϕ and

World Academy of Science, Engineering and Technology
International Journal of Industrial and Manufacturing Engineering
Vol:5, No:4, 2011

γ which is the included angle between $\mathbf{x_p}$ and $\mathbf{u}$ as

$$\gamma = \tan^{-1}(\tan\beta / \tan\alpha)$$

and $\mathbf{u}$ is the unit vector on $x_p y_p -$ plane with expression in $\mathbf{x_p y_p z_p}$ as

$$\mathbf{u} = < \cos\gamma \quad \sin\gamma \quad 0 >$$

From above, the tool axis $\mathbf{t}$ is assumed as rotating $\mathbf{n}$ by an angle ϕ about $\mathbf{u}$ in counterclockwise, and is obtained by homogeneous transformation matrix method [13], [14] with expression in $\mathbf{x_p y_p z_p}$ as

$$\mathbf{t} = < \sin\gamma \sin\phi \quad -\cos\gamma \sin\phi \quad \cos\phi >$$

Hence the local tool coordinate system represented by $\mathbf{x_T y_T z_T}$ can be completely determined where $\mathbf{z_T}$ is the same as $\mathbf{t}$, $\mathbf{x_T}$ is defined as the negative direction of $\mathbf{u}$, and $\mathbf{y_T} = \mathbf{z_T} \times \mathbf{x_T}$. The origin with $\mathbf{x_T y_T z_T}$ is by shifting O_p with a specific distance on $y_T z_T -$ plane. The $y_T z_T -$ plane can be applied to 3D tool compensation for postprocessor development of 5-axis machine centers [15]–[17].

For maintaining the tangent property in machining, the tool tip is translated by offsetting that depended upon tool orientation. Based on DIN 66215 [18] as Fig. 2 shows, a milling tool can be represented with geometric parameters as: d (tool diameter), r (fillet radius), e (horizontal distance), f (vertical distance), a (angle between horizontal and face), b (angle between vertical and generating line) and L (tool length).

Tung and Tso [19] had derived a generalized equation to represent each CC location $P(y_p, z_p)$ on the tool edge as

$$y_P(h) = (p_2^Y h^2 + p_1^Y h + p_0^Y)/(q_2^Y h^2 + q_1^Y h + q_0^Y) \qquad (2)$$

$$z_P(h) = (p_2^Z h^2 + p_1^Z h + p_0^Z)/(q_2^Z h^2 + q_1^Z h + q_0^Z) \qquad (3)$$

where h is defined as $\tan(\theta/2)$ and can be determined by inclination angle in (1). The origin is assumed to CL. Thus the offsetting distance can be obtained in a generalized form by (2) and (3). The normal vector $\mathbf{n}$ on the tool edge at the point P in y- and z-directions are given by

$$N_y(h) = -\sin\phi = (a_2^Y h^2 + a_0^Y)/(b_2^Y h^2 + b_0^Y) \qquad (4)$$

$$N_z(h) = \cos\phi = (a_1^Z h + a_0^Z)/(b_2^Z h^2 + b_0^Z) \qquad (5)$$

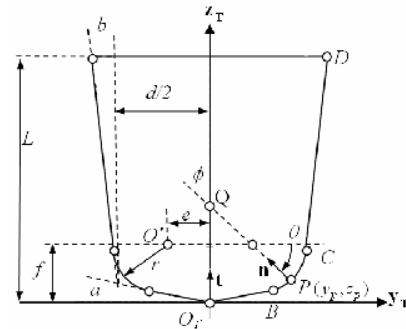where all coefficients in (2) to (5) are shown in Table I.

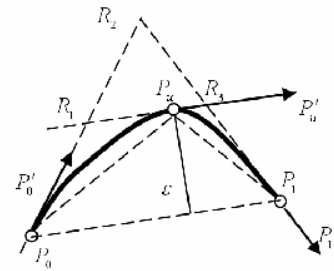Fig. 2 Geometric parameters of milling tool

Fig. 3 Curve by triangle partition

Therefore correlation between the CC point and the tip is obtained to perform tool path planning. For achieving better cutting performance, cutting locations with same θ should be avoided to prolong tool life and the spindle rotation should vary inversely with $y_p(h)$ as in (2)—the distance between the tool axis and CC points—to maintain stable cutting velocity.

III. LINEAR INTERPOLATION FOR CURVE SEGMENTS

A surface model can be reconstructed from measured data as a point cloud acquired by measurement. How to create a continuous and smooth curve through a set of given points is an essential issue for complex shape design. In order to define a free-form curve with segments, it is important to decompose the curve in parametric form. A cubic curve with C^2 continuity is wildly used and satisfied with most application. Many curve definitions such as Ferguson's, Bézier's, B-spline, and NURBS curves had developed to approximate the polygon linked by a series of control points [20], [21]. In this section an interpolation procedure will be introduced to generate the tool path for computation. Because the tool path in machine motion is along a point-to-point straight line, the objective of the partition is to generate a minimum deviation height that is within the tolerance limit. One of the segments between two successive points is as Fig. 3 shows. Let P_0 and P_1 be two endpoints, and P_0' and P_1' be the corresponding tangent directions with unit length. P_u is the point with the maximum chordal deviation ε in parabola. P_u' is the tangent direction with unit length parallel to $\mathbf{P_0 P_1}$.

A triangle partition discriminant is presented in (6) for approximating a degenerated curve into line segments by

World Academy of Science, Engineering and Technology
International Journal of Industrial and Manufacturing Engineering
Vol:5, No:4, 2011

interpolation. Each intersection points R_i is computed by tangent estimation to and then the area of each triangle is calculated. The division stops ideally when endpoints match together or chordal deviation approaches to zero.

$$
\begin{aligned}
\min(area\ P_0 P_1) &= \min(areaP_0 P_u + areaP_u P_1) \\
&= \min(P_0 R_1 R_3 P_1 - \Delta P_0 R_1 P_u - \Delta P_u R_3 P_1) \quad (6) \\
&= \min(\Delta P_o P_u P_1) = \min(\varepsilon \cdot |P_0 P_1|)
\end{aligned}
$$

.

where ε is the allowable tolerance, and the distance $|P_0 P_1|$ as step-length will be introduced in next section.

IV. TOOL PATH GENERATION FOR SCULPTURED SURFACE

A. Coordinate Systems of Cutting Layers

In CAM work for sculptured surface, machining surface is sliced into layers by a number of consecutive cutting planes. Tool path is generated with the contour pattern by the intersection of corresponding cutting layer and workpiece surface. Helical and z-constant patterns are wildly applied in tool-path generation topology. Scallop height and chordal deviation are used to determine the distance increment and step interval on layers for approximating the curve by line segments.

Castagnetti, Duc, and Ray [22] introduced the domain of admissible orientation concept to express the transformation between local and global systems. In this section, three coordinate systems as Fig. 4 shows are modeled and implemented for 5-axis manufacturing technology. The machine coordinate system represented by $x_M y_M z_M$ is for driving machine motion. The workpiece coordinate system represented by $x_W y_W z_W$ is for describing the geometry of workpiece in CAD planning. Unlike in 3-axis machining, the orientation of $x_W y_W z_W$ is varied with two rotation movements in 5-axis machine centers. Therefore postprocessors for different types of machines are developed as an interface that transforms CL data into machine controller data.

The part coordinate system represented by $x_P^i y_P^i y_P^i$, mentioned in section 2, is for each CC point along tool path in CAM planning where z_P^i is the surface normal and x_P^i is the instant feed direction toward to next CC point.

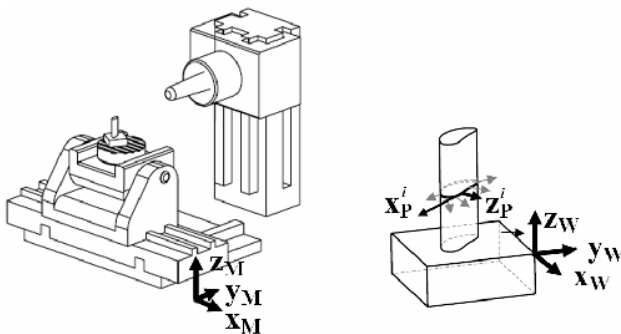Fig. 4 Coordinate frames in CAD/CAM system
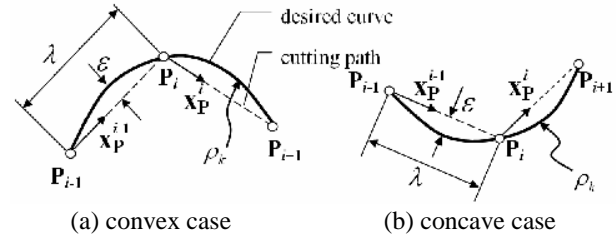

(a) convex case (b) concave case
Fig. 5 Step length and cutting tolerance

The localized L/T angles at each location on the surface belong to the variable user-control parameters. Lead angle is specified from the surface normal with respect to the tool travel direction where positive value drives the tool forward and negative drives backward. Tilt angle is together with lead angle where positive drives the tool to the right and negative to the left. As the tool moves between explicit axis definitions, the transformation from $x_P^i y_P^i y_P^i$ into $x_W y_W z_W$ can be derived in CAM system or by linear-interpolation computing immediately and precisely.

B. Cutter Interference Discriminant

Tool orientation plays an important role in 5-axis machining. Collision, overcut and abrupt variation should be prevented during machining. Because the tool axis is relative to the surface normal, the cutter orientation should be restricted in an adequate range for avoiding local interference.

Many deviation minimization principles [23]–[25] had been discussed to find an admissible tool size and to reposition the cutter center. Austin, Jerard, and Drysdale [26] provided an algorithm for surface discretization. The step-length λ is with restriction as

$$
\lambda \le \frac{2\rho_k}{(\rho_k + \rho_c)} \sqrt{\tau(2\rho_k + 2k\rho_c - \tau)} \quad (7)
$$

where ρ_k is the radius of normal curvature in the direction of the next point, ρ_c is the cutter radius with ball-end miller, and τ is the input tolerance. Besides, $k = 1$ is taken for a convex region and $k = -1$ is for concave.

As Fig. 5 shows, P_{i-1}, P_i, and P_{i+1} are assumed as previous, present and next cutting locations respectively. ρ_c can be assigned by the distance between tip and CC location through (2) and (3). Hence the deviation partition in (6) can be utilized by substituting parameter λ that can be defined through (7) to implement the ideal linear interpolation for tool path generation.

A manufacturing procedure that consists of model reconstruction, tool orientation assignment, CC location continuity, interference detection, CL-data computation, cutting region classification, and operation stage systematization is in flowchart form as Fig. 6 shows. An example for machining blades will be presented in the following.
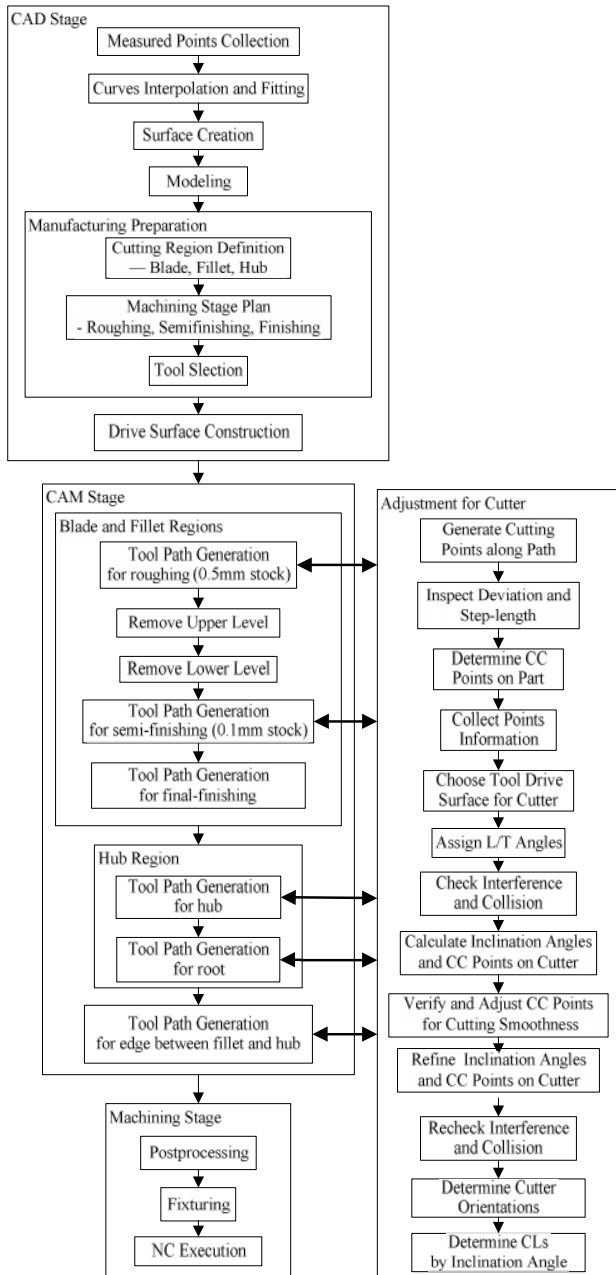
World Academy of Science, Engineering and Technology
International Journal of Industrial and Manufacturing Engineering
Vol:5, No:4, 2011

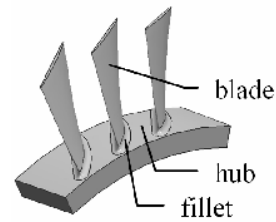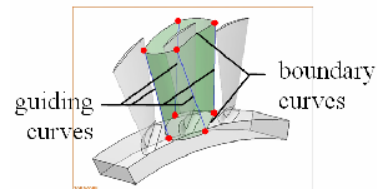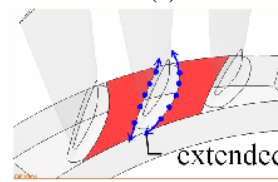Fig. 6 Manufacturing procedure

Fig. 7 Geometric modeling of blades

(a) for blade and fillet regions

(b) for main hub region   (c) for residual hub region

Fig. 8 Drive surfaces for blade

In the tool path planning for blades, the tool orientation can be calculated by L/T angles relative to the surface normal for every CC point that had been identified in section 2. However the blade surface is often with complex shape, curvatures on path might vary sharply at locals. In this research a drive-surface method is proposed to restrain excessive inclination of the cutter for obtaining the better tool path.

B. Drive Surfaces for Blade Machining

The purpose of using drive surface is not only to prevent the poor smoothness and continuity caused from model surface but also to compel the cutter in desired orientations. There are two suggestions for drive surface construction. First, the boundary curves could mainly inherit the original edges that can be obtained through the control points on the intersection between workpiece surfaces. Second, the guiding curve that aids blending boundary curves to build the ruled surface could be represented by a known equation in analytical expression.

Drive surface for manufacturing blade and root regions is based on the blade shape as Fig. 8(a) shows. The top and bottom boundary curves are both composed by four curve segments. Two curves are offset from free-form contours that are generated from the simplified edges; another two are created from separate fillets tangent to two previous curves. The guiding curves are all straight lines that connected by endpoints of top and bottom boundary curves. Hence drive surface for blade is built by blending two boundary contours along four straight guiding lines.

V. MANUFACTURING PROCESS FOR TURBINE BLADE

A. Geometric Modeling for Blades of Impeller

The modeling of blades, as Fig. 7 shows, composed of three regions: blade, fillet and hub. Information about workpiece, such as a series of cloud-of-points data, is often collected by measurement. Then a shape model can be constructed through those control points by inverse engineering technology.

Machining sequence for impeller regions in this paper is characterized into three as blade, hub and remainder-removal. Due to the axisymmetric property of blades, the toolpath for each cutting stage is edited for one blade only. Then the rotating function is used to translate the subprogram for simplification.

World Academy of Science, Engineering and Technology
International Journal of Industrial and Manufacturing Engineering
Vol:5, No:4, 2011

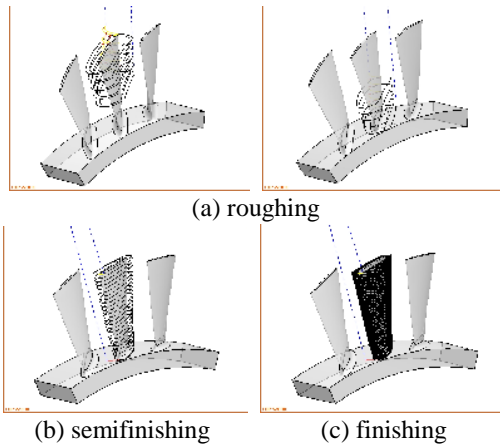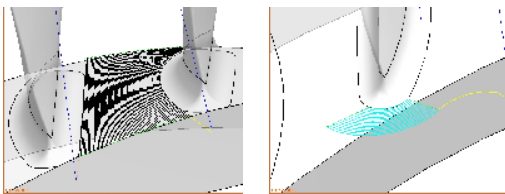(a) roughing

(b) semifinishing

(c) finishing

Fig. 9 Machining stages for blade and fillet

(a) zig-zag for cone   (b) circular for root

Fig. 10 Finishing regions for hub

Drive surfaces for hub are composed of two regions: a free-form surface for cone and a closed circular ring for removing residual. In Fig. 8(b), boundary curves are reconstructed and extended through the designate control points on the intersections; guiding curves are arcs from edges of hub. In Fig. 8(c), drive surface for closed ring is between intersection and offsetting boundary curves.

C. Cutting Stages of Operation

For achieving better surface accuracy and quality, machining operation is separated into two parts by five NC subprograms: one drive surface as Fig. 8(a) shows is applied to blade and fillet surfaces; two as shown in Fig. 8(b) and Fig. 8(c) are for hub. Blade surface milling is similar to side milling and hub surface machining is similar to end milling. Root milling is similar to the combination of side and end milling. The operation stages for blade are arranged into roughing, semifinishing and finishing. Raw stock is as disk-shape. The purpose on roughing is as slotting—removing most spare material and remaining 0.5mm stock for the following processes. Two levels in roughing with end-milling are shown in Fig. 9(a). Semifinishing, as Fig. 9(b) shows, generates in 25 layers and provides 0.1mm stock to preform-surface for finishing. And final finishing for each blade and fillet, generating in 125 layers with one single pass by a ball-end cutter, is executed as Fig. 9(c) shows. The default L/T angles are 85 and 3 degree respectively. Because the cut-across widths along cutting direction on hub surface are different, the stepover distances are not the constant. For saving machine time and improving surface quality, two regions are divided as Fig. 10 shows for hub machining. The stepovers for cone and root are 60 and 16 respectively. In the tool vector definition on hub

surface, the tool axis needs to be inclined to the surface normal for avoiding zero-velocity cutting. Tool axis assignment can be interpolated through four guiding lines as Fig. 8(a) shows. Last, the intersection edge between fillet and hub surfaces is machined with one single pass by a ball-end cutter of the tool-radius smaller than the fillet radius for visual inspection.

VI. CONCLUSION

This paper deals with the tool path generation and 5- axis machining for a compressor rotor with blades. The cutting point on the milling tool is acquired directly and the distance from the tip to the contact location is calculated exactly by a generalized equation. By means of chordal deviation and step-length restriction, linear interpolation can be implemented flexibly to enhance surface accuracy. Smoothness and continuity of tool orientations is controlled by drive surface method underneath interference detection. Adjustment for CC locations can be triggered to prolong tool life by assigning inclination angle. Tool path is eventually generated to accomplish rotor manufacturing.

REFERENCES

[1] E. L. J. Bohez, S. D. R. Senadhera, K. Pole, J. R. Duflou, and T. Tar, "A geometric modeling and five-axis machining algorithm for centrifugal impellers," *J. Manuf. Syst.*, vol. 16, pp. 422–436, 1997.
[2] E. Buduk, "Improving productivity and part quality in milling of titanium based impellers by chatter suppression and force control," *Ann. CIRP.*, vol. 49, pp. 31–36, 2000.
[3] T. S Lim, C. M. Lee, S. W. Kim, and D. W. Lee, "Evaluation of cutter orientations in 5-axis high speed milling of turbine blade," *J. Mater. Process Technol.*, vol. 130-131, pp. 401–406, Dec. 2002.
[4] C. J. Chiou and Y. S. Lee, "A shape-generating approach for multi-axis machining G-buffer models," *Comput. Aided D.*, vol. 31, pp. 761–776, Oct. 1999.
[5] C. G. Jensen, W. E. Red, and J. Pi, "Tool selection for five-axis curvature matched machining," *Comput. Aided D.*, vol. 34, pp. 251–266, Mar. 2002.
[6] C. S. Jun, K. Cha, and Y. S. Lee, "Optimizing tool orientations for 5-axis machining by configuration-space search method," *Comput. Aided D.*, vol. 35, pp. 549–566, May 2003.
[7] J. Chaves-Jacob , G. Poulachon, and E. Ducb, "New approach to 5-axis flank milling of free-form surfaces: computation of adapted tool shape," *Comput. Aided D.*, vol. 41, pp. 918–929, Dec. 2009.
[8] S. P. Radzevich, "Conditions of proper sculptured surface machining," *Comput. Aided D.*, vol. 34, pp. 727–740, Sep. 2002.
[9] P. Gilles, F. Monies, and W. Rubio, "Optimum orientation of a torus milling cutter: method to balance the transversal cutting force," *Int. J. Mach. Tools Manuf.*, vol. 47, pp.2263–2272, Dec. 2007.
[10] K. L. Chui, W. K. Chiu, and K. M. Yu, "Direct 5-axis tool-path generation from point cloud input using 3D biarc fitting," *Robot Comput. Integr. Manuf.*, vol. 24, pp. 270-286, Apr. 2008.
[11] B. Lauwers, P. Dejonghe, and J. P. Kruth, "Optimal and collision free tool posture in five-axis machining through the tight integration of tool path generation and machine simulation," *Comput. Aided D.*, vol. 35, pp. 421-432, Apr. 2003.
[12] E. Ozturk, L. T. Tunc, and E. Budak, "Investigation of lead and tilt angle effects in 5-axis ball-end milling processes," *Int. J. Mach. Tools Manuf.*, vol. 49, pp. 1053-1062, Nov. 2009.
[13] J. Denavit and R. S. Hartenberg, "A kinematic notation for lower-pair mechanisms based on matrices," *J. Appl. Mech.*, vol. 22, pp. 215–221, 1955.
[14] B. K. Choi and R. B. Jerard, *Sculptured Surface Machining Theory and Applications*, Kulwer Academic, 1998, pp. 26-30.

World Academy of Science, Engineering and Technology
International Journal of Industrial and Manufacturing Engineering
Vol:5, No:4, 2011

[15] G. Erdos, M. Muller, and P. Xirouchakis, "Parametric tool correction algorithm for 5-axis machining," *Adv. Eng. Softw.*, vol. 36, pp. 654-663, Oct. 2005.

[16] E. L. J. Bohez, "Five-axis milling machine tool kinematic chain design and analysis," *Int. J. Mach. Tools Manuf.*, vol. 42, pp. 505–520, Mar. 2002.

[17] C. Tung and P. L. Tso, "Inverse kinematics with 3-dimensational tool compensation for 5-axis machine center of tilting rotary table," *2011 2nd Int. Conf. MIMT*, Singapore, Feb., to be published.

[18] DIN, *DIN 66215: CLDATA. NC-Maschinen*, Berlin, Beuth Verlage, 1987.

[19] C. Tung and P. L. Tso, "A generalized cutting location expression and postprocessors for multi-axis machine centers with tool compensation," *Int. J. Adv. Manuf. Technol.*, vol. 50, pp. 1113–1123, Oct. 2010.

[20] L. Piegl and W. Tiller, *The NURBS Book*, Springer, 1995.

[21] T. C. Chang, R. A. Wysk, and H. P. Wang, *Computer-Aided Manufacturing*, 2nd ed., Prentice Hall, 1998, pp. 369-378.

[22]

C. Castagnetti, E. Duc, and P. Ray, "The domain of admissible orientation concept: a new method for five-axis tool path optimisation," *Comput. Aided D.*, vol. 40, pp. 938–950, Sep. 2008.

[23] R. Gian, T. W. Lin, and A. C. Lin, "Planning of tool orientation for five-axis cavity machining," *Int. J. Adv. Manuf. Technol.*, vol. 22, pp. 150-160, Sep. 2003.

[24] Y. K. Choi, A. Banerjee, and J. W. Lee, "Tool path generation for free form surface using Bézier curves/surfaces," *Comput. Ind. Eng.*, vol. 52, pp. 486-501, May 2007.

[25] H. Gong and N. Wang, "Optimize tool paths of flank milling with generic cutters based on approximation using the tool envelope surface," *Comput. Aided D.*, vol. 41, pp. 981–989, Dec. 2009.

[26] S. Austin, R. B. Jerard, and S. Drysdale, "Comparison of discretization algorithms for NURBS surfaces with application to numerically controlled machining," *Comput. Aided D.*, vol. 29, pp. 71-83, Jan. 1997.

TABLE I
COEFFICIENTS IN GENERALIZED EXPRESSIONS

Item	Tip	Bottom	Arc	Side	Item	Tip	Bottom	Arc	Side
		Coefficients about Point P in Numerator					Coefficients about Point P in Denominator		
p_2^Y	0	f	$e-r$	$f\tan b + d(1-\tan a\tan b)/2$	q_2^Y	0	$\tan a$	1	1
p_1^Y	0	$-2e$	0	$-2e\tan\beta$	q_1^Y	0	-2	0	$-2\tan b$
p_0^Y	0	$-f$	$e+r$	$-f\tan b - d(1-\tan a\tan b)/2$	q_0^Y	1	$-\tan a$	1	-1
p_2^Z	0	f	f	f	q_2^Z	0	1	1	1
p_1^Z	0	$-2e$	$-2r$	$d(1-\tan a\tan b)-2e$	q_1^Z	0	$-2\cot\alpha$	0	$-2\tan b$
p_0^Z	0	$-f$	f	$-f$	q_0^Z	1	-1	1	-1
a_2^Y	0	0	1	0	b_2^Y	0	0	1	0
a_0^Y	0	$-\sin a$	-1	$-\cos b$	b_0^Y	1	1	1	1
a_1^Z	0	0	2	0	b_2^Z	0	0	1	0
a_0^Z	1	$\cos a$	0	$\sin b$	b_0^Z	1	1	1	1